

The conformation of membranes

Reinhard Lipowsky

Membranes composed of amphiphilic molecules are highly flexible surfaces that determine the architecture of biological systems and provide a basic structural element for complex fluids such as microemulsions. Physical theories have been developed to describe many aspects of their conformational behaviour, such as the preferred shapes and shape transformations of closed vesicles, and the shape fluctuations, random-surface configurations, and adhesion and unbinding of interacting membranes. Understanding of these phenomena has been much improved through fruitful interactions between theory and experiment.

THE membranes that I shall consider here are very thin and highly flexible sheets of amphiphilic molecules—structures that are a ubiquitous component of biological systems. On length scales large compared with the size of the molecules, these membranes can be regarded as two-dimensional surfaces embedded in three-dimensional space. The behaviour of these surfaces has recently attracted interest from several communities.

Biology, biophysics and biochemistry. Membranes represent the main structural component for the complex architecture of biological systems. The human brain, for example, consists of a complex network of membranes with a total surface area of $10^3\text{--}10^4 \text{ m}^2$. Biophysicists have constructed a number of model membranes that are expected to capture some of the essential features of their biological counterparts. The simplest models of this kind are provided by lipid bilayers which assemble spontaneously from lipid molecules dissolved in water.

Physical chemistry and chemical engineering. Surfactant molecules in mixtures of immiscible fluids often assemble into membranes which then form a variety of different structures. These supramolecular structures can include: a liquid crystal such as a smectic phase formed by an ordered stack of membranes; a periodic crystal in which the membranes divide space into two interpenetrating labyrinths and thus form a bicontinuous structure; or new, unusual phases such as the so-called sponge phase, which represents a bicontinuous but disordered state of matter.

Theoretical physics and mathematics. To understand the conformational behaviour of membranes, one has to introduce a number of novel theoretical concepts such as bending elasticity and curvature, scale invariance arising from fluctuations on many length scales, and renormalization of membrane interactions. I will try to explain these theoretical concepts and their relation to experiments. One intriguing aspect of this topic is the need to combine mathematical techniques such as differential geometry (see Box A) and renormalization group theory (see Box B) with the behaviour of real systems as observed under the microscope.

Mesoscopic shape of membranes

In aqueous solution, lipid or surfactant bilayers typically form closed surfaces or vesicles. Multilamellar vesicles consisting of several phospholipid bilayers were first observed by electron microscopy¹. Several methods are now available through which one can obtain large unilamellar vesicles consisting of a single lipid bilayer². Such vesicles have a linear size of the order of 1–10 μm and can be studied directly by optical microscopy. These observations have shown that lipid vesicles exhibit a large variety of different shapes (Fig. 1a, b); in particular, they can exhibit the non-spherical, biconcave shape typical of red blood cells^{3,4}.

Bending elasticity and formation of vesicles. It is well known that liquid droplets usually have a spherical shape which is governed by interfacial tension. Non-spherical shapes cannot be determined by such a tension. It is now generally believed that the shape of vesicles is determined primarily by bending

elasticity and curvature^{5–7}. This idea leads to the theoretical model described in Box A. In this model, which I will call the curvature model, the energy of a given shape depends on the mean curvature and on the gaussian curvature of the membrane⁶ (see Box A). In its simplest version, this model involves only two parameters: the bending rigidity, κ , and the gaussian curvature modulus, κ_G . For phospholipid bilayers, $\kappa \approx 10^{-19} \text{ J}$ (refs 8, 9).

One nice feature of the curvature model is that it provides a very simple explanation for the fact that bilayers tend to form vesicles. Consider a membrane segment of linear size L . If this segment is planar, it has no bending energy but its boundary has an edge energy, σ_E , per unit length arising from the partial contact between the water and the hydrocarbon chains of the lipid. The total edge energy of the segment is thus proportional to L . On the other hand, if the segment forms a sphere, it has no edge energy but the bending energy is non-zero, and is given

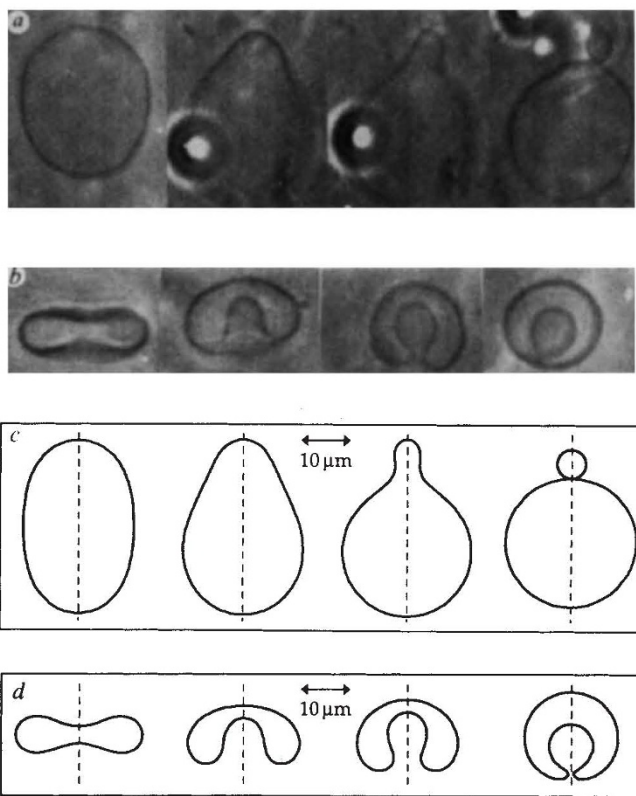


FIG. 1 Shape transformations of free vesicles induced by a change in temperature⁴. a, c, Expulsion of a small vesicle from a larger one (budding). b, d, Inverse budding ('endocytosis') via the transformation from a discocyte to a stomatocyte. The shapes are axisymmetric with respect to the broken line.

by $4\pi(2\kappa + \kappa_G)$, which does not depend on the linear size L of the membrane (see Box A). Therefore, for large L , the membrane can always lower its energy by forming a closed surface. For phospholipid bilayers, the edge energy $\sigma_E \approx 10^{-20} - 10^{-19} \text{ J nm}^{-1}$ (refs 10, 11). This mechanism of vesicle formation via the hydrophobic effect is quite general, and operates in biological systems which usually contain a large number of such structures.

Shape transformations of free vesicles. Consider again the vesicle shapes shown in Fig. 1a and b. These micrographs show a single lipid vesicle, which undergoes shape transformations induced by a change in temperature.

In thermal equilibrium, the vesicle should attain the shape that corresponds to the minimum bending energy. If one assumes rotational symmetry, these minimal shapes can be calculated from the curvature model¹²⁻¹⁴. It has been found recently that, if one assumes that the two monolayers of the bilayer exhibit a small asymmetry^{4,14}, the experimentally observed shapes and shape transformations shown in Fig. 1a and b can be explained by such minimal shapes (Fig. 1c, d).

Adhesion of vesicles and vesicle fusion. Now consider a vesicle that interacts with another membrane or surface. If this interaction is attractive, it can lead to a bound state of the vesicle. Bound states have been investigated experimentally by micropipette techniques¹⁵, which allow one to study, for example, the adhesion of two vesicles (Fig. 2).

Box A. DIFFERENTIAL GEOMETRY AND THE CURVATURE MODEL

Consider a two-dimensional surface embedded in three-dimensional space. At each point on the surface, one can define two principal curvatures, C_1 and C_2 , which determine the mean curvature $C_1 + C_2$ and the gaussian curvature $C_1 C_2$. The curvature model is then defined by the configurational energy or 'effective Hamiltonian'⁶

$$\mathcal{H} = \oint dA \left\{ -\kappa C_0(C_1 + C_2) + \frac{1}{2}\kappa(C_1 + C_2)^2 + \kappa_G C_1 C_2 \right\} \quad (\text{A.1})$$

where the integral extends over the whole membrane surface (which could consist of several disconnected components) and dA represents the intrinsic area element. The parameters κ , C_0 and κ_G are the bending rigidity, spontaneous curvature and gaussian curvature modulus, respectively. For a symmetric membrane (both sides identical), $C_0 = 0$.

The shape of a vesicle with surface area A and enclosed volume V is determined by minimization of $\mathcal{H} + PV + \Sigma A$, where P and Σ denote the difference between the outside and the inside pressure and the lateral tension, respectively. For phospholipid bilayers, the exchange of lipid molecules with the surrounding solution is very slow and the area A is essentially constant on experimentally relevant timescales. In addition, one may control the vesicle volume V , for example by varying the concentration of a solute that cannot permeate the bilayer. The pressure P and the tension Σ then play the role of Lagrange multipliers. This approach has been used to calculate the shapes shown in Fig. 1 and Fig. 3.

For a spherical vesicle of radius R , $|C_1| = |C_2| = R$. When inserted into (A.1) with $C_0 = 0$, one obtains $\mathcal{H} = 4\pi(2\kappa + \kappa_G)$. In fact, for a closed surface, the third term in (A.1) always leads to a constant that does not depend on the size of the surface but only on its topology or, more precisely, on its Euler characteristic⁹⁶, χ . For a surface without edges, the integral over the gaussian curvature is given by

$$\oint dA C_1 C_2 = 2\pi\chi \quad (\text{A.2})$$

as follows from the Gauss-Bonnet theorem of differential geometry⁹⁶.

Now consider the minimal surface shown in Fig. 4b, for which the mean curvature, $C_1 + C_2$, is zero everywhere. This surface is topologically equivalent to a cubic lattice of spheres connected in all three spatial directions by pieces of cylinders; it has Euler characteristic $\chi = -4$ per lattice site. Thus, for $C_0 = 0$, the bending energy of the minimal surface in Fig. 4b is given by $\mathcal{H} = -8\pi\kappa_G$ per lattice site. The same energy applies, for $C_0 \neq 0$, to a surface with constant $C_1 + C_2 = C_0$. The latter surface represents a minimum of $\mathcal{H} + PV + \Sigma A$; it thus represents a model for the prolamellar body shown in Fig. 4a.

The shape of a bound vesicle is determined by the interplay between adhesion and bending energies. This interplay can be studied theoretically by starting from a simple generalization of the curvature model in which the membrane experiences a contact potential arising from the attractive surface^{16,17}. If one assumes that the vesicle does not change its topology, theory predicts a large variety of different bound states (Fig. 3). As shown in this figure, the vesicle can undergo shape transformations between free and bound states as well as transformations between different bound states.

Adhesion can also lead to topological changes such as vesicle rupture and vesicle fusion. In the limit of strong adhesion, a bound vesicle with constant volume attains the shape of a spherical cap. In this limit, the adhesion energy, E_{ad} , is related to the lateral tension Σ by the Young-Dupre equation: $E_{ad} = \Sigma(1 + \cos \psi_{eff})$, where ψ_{eff} denotes an effective contact angle^{16,17}. If the tension Σ exceeds a certain threshold, it will disrupt the membrane. As a result, the closed vesicle will be transformed into a disk-like membrane segment with a free edge. A segment of linear size L has an adhesion energy proportional to L^2 , which overcomes the edge energy (proportional to L) for sufficiently large L .

If two vesicles collide, they may adhere and eventually fuse into a larger one¹⁸. According to the curvature model, the energy gained by the fusion of two free vesicles is $\Delta E = 4\pi(2\kappa + \kappa_G)$ ¹⁹. Thus, fusion of two free vesicles is energetically favourable if $\kappa_G > -2\kappa$. In principle, the fusion process also involves a loss of translational entropy which leads to a free-energy increase of the order of $kT \ln(R/L)$ where R and L are the linear sizes

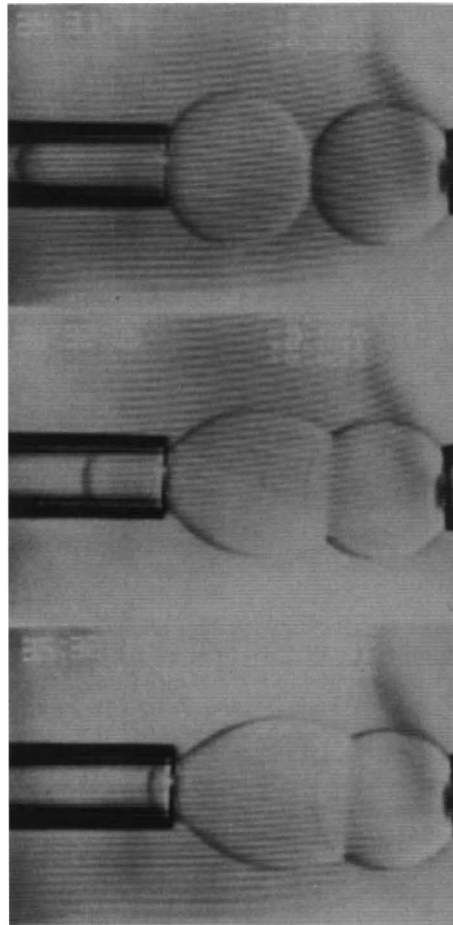


FIG. 2 Adhesion of two lipid vesicles which are brought into contact by two micropipettes. The vesicle radii are $\approx 10 \mu\text{m}$ (courtesy of E. Evans).

of the container and of the vesicle respectively (k is the Boltzmann constant). For lipid bilayers with $\kappa \approx 10-20 kT$, this entropic contribution is usually small relative to the bending energies.

On the other hand, for two bound vesicles of linear size L , the energy gained by fusion is proportional to L for large L (ref. 17). Therefore, two vesicles can fuse in their bound state even if they cannot fuse in their free state. Such an adhesion-induced fusion process has been observed for vesicles attracted by a gold surface²⁰ and for lecithin membranes at the air-water interface²¹.

Ordered and disordered assemblies of bilayers. So far, I have discussed the behaviour of one or two vesicles in plenty of water. For a larger concentration of amphiphilic molecules, membranes can assemble into a variety of different structures. First, the membranes may spontaneously form an ensemble of unilamellar vesicles, as has been observed for bilayers of several kinds of surfactant²²⁻²⁵. Lipid bilayers, on the other hand, often form layered structures such as multilamellar vesicles, myelin cylinders or oriented stacks, which are stabilized by interactions between the membranes.

Another possible structure is a triply periodic surface which divides the whole three-dimensional space into two interwoven labyrinths or subvolumes and thus gives rise to a bicontinuous phase²⁶⁻³⁰. Such crystalline states of bilayers have been reported for a variety of amphiphilic molecules^{27,29,30} and are present in plant cells²⁶ (Fig. 4a). In some cases, the partitioning bilayer forms a 'minimal surface', which is characterized by zero mean curvature. An example with cubic symmetry is shown in Fig. 4b. Minimal surfaces can exhibit many different symmetries, and there has been recent progress in classifying the corresponding space groups³¹. Triply periodic surfaces with constant but non-zero mean curvature have also been constructed^{32,33}.

The ordered structures shown in Fig. 4a and b are perturbed by thermally excited shape fluctuations of the bilayers. These fluctuations can pinch off some of the narrow necks and can introduce other types of defects, causing the crystals to melt into a sponge phase (Fig. 4c). A sponge phase, which is still bicontinuous but exhibits no long-range order, seems to have been observed for surfactant bilayers³⁴⁻³⁶. This interpretation is still somewhat controversial: an alternative model in terms of disk-like membrane segments has also been proposed (C. A. Miller *et al.*, preprint, Univ. of Bayreuth).

Shape fluctuations of membranes

In general, low-dimensional objects such as interfaces, membranes and polymers undergo thermally excited shape fluctuations to increase their configurational entropy³⁷. A membrane is usually more flexible than an interface but less flexible than a polymer. It has been realized recently that the character of its shape fluctuations depends on the internal state of the membrane, which can be fluid, polymerized or hexatic (see below).

The shape fluctuations of a lipid vesicle can be observed directly under a light microscope. In this way, one can probe fluctuations with wavelengths of the order of the vesicle radius. It is important to realize, however, that these fluctuations involve a large range of different length scales, from molecular dimensions up to the membrane size, most of which cannot be resolved by the microscope.

In the following, I will assume that there is essentially no reservoir of amphiphilic molecules within the aqueous solution—in other words, that these molecules have all assembled into bilayers. This should apply to lipids and double-chained surfactants that have a very low critical micelle concentration. One is thus led to study the shape fluctuations of random surfaces that contain a fixed number of molecules.

Fluid membranes. Biological membranes are typically fluid³⁸, which means that the molecules can diffuse rapidly within the membrane. This fluidity was first recognized in experimental studies of lipid bilayers³⁹. At sufficiently high temperatures,

these bilayers exhibit a fluid phase with a diffusion constant $D \approx 10^{-7}-10^{-8} \text{ cm}^2 \text{ s}^{-1}$ (ref. 40).

The molecules within a fluid membrane possess no reference lattice. In the absence of lateral tension, the shape of the membrane is then governed by its bending rigidity, κ , and the shape fluctuations represent bending modes. These modes lead to a certain roughness: at temperature T , a membrane segment of linear size L forms spatially anisotropic humps of transverse extension $L_\perp \sim (kT/\kappa)L$ (ref. 41). On the other hand, if one applies a lateral tension, Σ , the membrane roughness is strongly reduced and $L_\perp \sim (kT/\Sigma)^{1/2}[\ln(L/a)]^{1/2}$, where a is a microscopic length scale.

The shape fluctuations of tensionless fluid membranes represent a boundary case, because the overall gradient of the humps, L_\perp/L , does not decay for large L . In fact, it follows from the curvature model that the scaling behaviour $L_\perp \sim (kT/\kappa)L$ applies only for length scales L that are small compared with the so-called persistence length $\xi_p = a \exp[c\kappa/kT]$, where c is a dimensionless coefficient⁴². Furthermore, as L is increased towards ξ_p , the shape fluctuations reduce the bending rigidity and lead to an effective rigidity $\kappa_{\text{eff}} \approx \kappa - c'kT \ln(L/a)$ in the limit of small kT/κ (refs 43, 44).

For phospholipid bilayers at room temperature, the persistence length ξ_p is usually much larger than the size of the membranes, and the reduction of the bending rigidity by shape fluctuations is negligible. An exceptionally small value for ξ_p is obtained for lecithin membranes containing a small amount of bipolar ('bola') lipid, leading to $\kappa_{\text{eff}} \approx kT$ (ref. 8). Such values for κ_{eff} may also apply to surfactant bilayers that form lamellar and bicontinuous phases⁴⁵⁻⁴⁷.

In general, the membrane should have an effective bending rigidity of the order of kT on length scales $L \approx \xi_p$. It will then undergo rather strong shape fluctuations. The character of these fluctuations is, however, not understood. Real membranes cannot self-intersect and this constraint of self-avoidance is difficult to treat theoretically. Recently, fluid-like membranes with self-avoidance have been investigated by computer simulation, but so far no (bare) bending rigidity has been included⁴⁸.

Three different possibilities can be envisaged for the large-scale behaviour of fluid membranes. (1) The membrane could become highly convoluted or crumpled: a membrane segment of linear size L forms spatially isotropic blobs of size $R \sim L'$

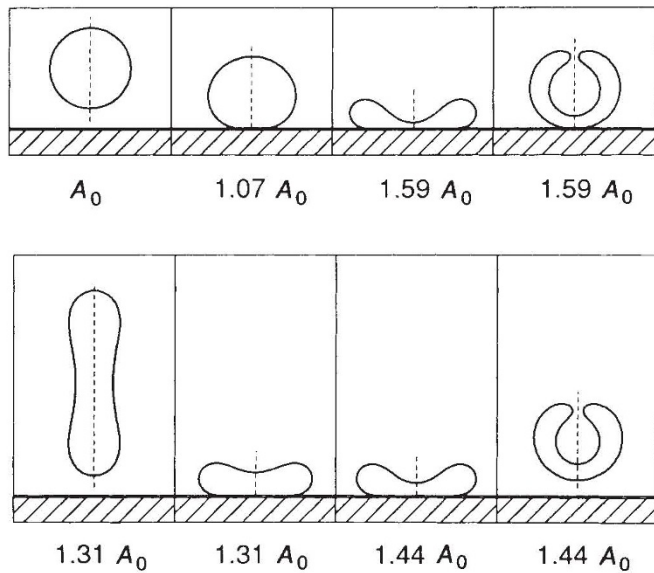


FIG. 3 Shape transformations of a vesicle interacting with a planar surface. These transformations are induced by a change in area at constant volume. The initial state is a sphere with area A_0 . The upper and the lower sequence correspond to two different contact potentials.

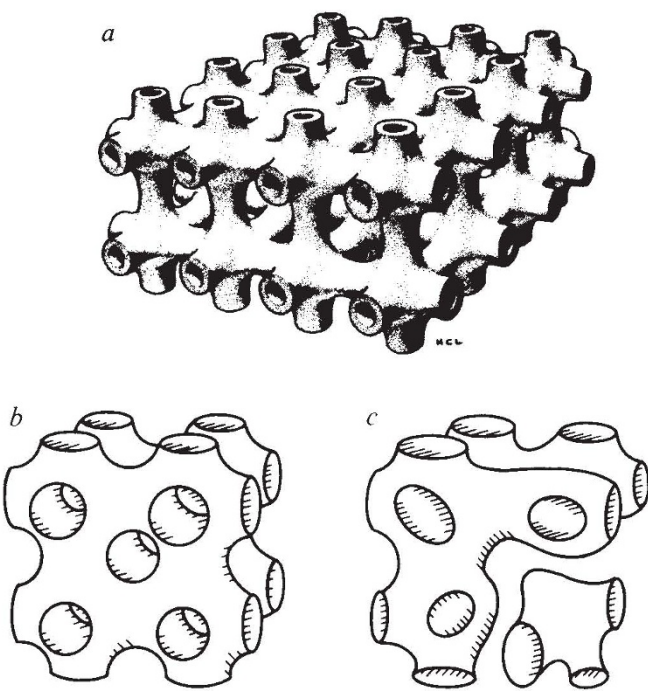


FIG. 4 Bicontinuous structures of bilayers. *a*, Prolamellar body as present in some organelles of plant cells²⁶. *b*, Triply periodic minimal surface. The mean curvature vanishes for each point of this surface. *c*, Sponge phase, obtained by melting of the bilayer crystals shown in *a* and *b*.

with $\nu \geq 0$. A crumpled membrane represents the two-dimensional analogue of a one-dimensional polymer chain^{49,50,57}. In fact, it has been speculated that crumpled fluid membranes exhibit the same scaling properties as branched polymers. This behaviour has been found for one-dimensional ring polymers ('planar vesicles') in two dimensions when deflated by an external pressure⁵¹. If two-dimensional fluid membranes in three dimensions indeed exhibit the same scaling behaviour as branched polymers, the crumpled blobs would scale as $R \sim L^\nu$ with $\nu \approx 1$ (ref. 37). (2) On the other hand, there is no clear evidence so far that self-avoiding fluid membranes governed by bending rigidity are indeed crumpled. Thus, it is possible that self-avoidance prevents crumpling and acts to stabilize the effective bending rigidity at the value $\kappa \approx kT$. (3) If the membrane is allowed to undergo topological changes, it could break up into smaller pieces (Fig. 4c). The energy required to create a spherical vesicle of size ξ_p is $\sim 8\pi kT$, which might be overcome by the translational entropy of the vesicle. Lecithin bilayers containing bipolar lipids might show this behaviour, as they have been seen to expel small vesicles on experimental timescales.⁸

Polymerized membranes. Biological membranes often contain two-dimensional protein networks, such as the spectrin network which is part of the plasma membrane of red blood cells⁵². As the timescales for breaking and reassembling the molecular connections of these networks are usually large compared with the timescales involved in the shape fluctuations⁷⁰, the networks can be regarded as 'fishnets' of fixed connectivity.

The mesh size of protein networks is typically large (~ 100 nm). Polymerized membranes with a much smaller mesh size can be obtained from bilayers of polymerizable lipids^{53,54}. Several types of lipids are now available that have two or more polymerizable units per molecule, polymerization of which can often be accomplished by irradiation of the bilayer with ultraviolet light.

On length scales that are large relative to the mesh size of the network, a polymerized membrane can be regarded as a thin elastic sheet. The shape fluctuations of such a sheet consist of both bending and stretching modes^{55,56}. For a phantom membrane with self-intersections, these shape fluctuations lead to a crumpled state: a membrane segment of linear size L forms blobs of lateral extension $R \sim a[\ln(L/a)]^{1/2}$, where a is a micro-

scopic length scale. For zero bending rigidity, a crumpled state exists for all non-zero temperatures⁵⁰. For finite bending rigidity ($\kappa > 0$), on the other hand, the phantom membrane undergoes a crumpling transition at a critical temperature $T = T_{cr}$ (Fig. 5)⁵⁷⁻⁵⁹. For $T > T_{cr}$, the bending rigidity is irrelevant and the membrane behaves as though $\kappa = 0$; for $T < T_{cr}$, the bending rigidity is relevant and the membrane exhibits a rough but uncrumpled state.

The rough state of a polymerized membrane is again characterized by anisotropic humps: a membrane segment of linear size L makes transverse excursions of size $L_\perp \sim L^\zeta$ (ref. 60). In contrast to fluid membranes with $\zeta = 1$, the roughness exponent ζ now satisfies $\zeta < 1$ and the overall gradient of the hump, $L_\perp/L \sim L^{\zeta-1}$, decays for large L . Computer simulations of

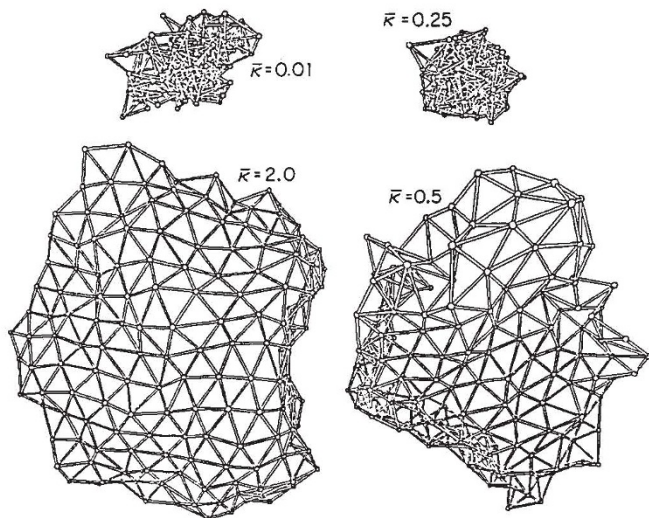


FIG. 5 Crumpling transition of a polymerized membrane with self-intersections, induced by a change in the reduced bending rigidity, $\bar{\kappa} = \kappa/kT$. For $\kappa/kT = 0.01$ and 0.25, the membrane is crumpled; for $\kappa/kT = 2.0$ and 0.5, the membrane is rough but not crumpled. The transition takes place at $\kappa/kT \approx 0.33$. (Courtesy of Y. Kantor and D. R. Nelson.)

tethered networks gave an estimate $\zeta = 0.65 \pm 0.05$ (refs 61, 62). More recently, Monte Carlo simulations of solid-like elastic sheets revealed that $\zeta = 1/2$, which is consistent with the existence of a finite shear modulus for the membrane on large scales⁶³.

As mentioned, a real membrane cannot intersect itself. This constraint of self-avoidance does not affect the rough state of a membrane but acts to prevent its crumpling. Recent simulations have shown that the tethered networks considered so far are not crumpled at any finite temperature as a result of self-avoidance^{64–66}.

Crystalline and hexatic membranes. At low temperature or high lateral pressure, monolayers and bilayers of surfactant or lipid molecules exhibit solid-like phases with translational short-range ordering of the molecules. One may often define two different reference lattices: one for the hydrocarbon chains and one for the polar head groups. The mismatch between these two lattices is expected to lead to a high density of defects, such as dislocations⁶⁷.

Another mechanism for the proliferation of dislocations is provided by buckling⁵⁶. For a flat membrane, a single dislocation has a stretching energy that diverges logarithmically with the membrane size. This energy can be reduced by buckling. Recent calculations indicate that, for a buckled membrane, the energy of such a dislocation might be finite⁶⁸. Dislocations would then be thermally activated and thus would melt the crystalline phase at any finite temperature. This could lead to a normal fluid phase, or alternatively to a hexatic phase—a kind of anisotropic fluid⁵⁶.

Theoretically, a hexatic membrane with self-intersections is found to exist at sufficiently low temperatures, characterized by a finite bending rigidity, κ_{eff} , on large scales⁶⁹. Such a membrane is less crumpled than a tethered membrane (with self-intersections). Therefore, hexatic membranes with self-avoidance are presumably not crumpled; their shape fluctuations should then be characterized by the roughness exponent $\zeta = 1$ (ref. 60).

Plasma membrane of red blood cells. On the molecular level, biological membranes are rather complex⁵². One such structure that has been studied extensively is the plasma membrane of red blood cells⁷⁰. This consists of two coupled membranes: a fluid bilayer which contains a mixture of many lipids and proteins, and a two-dimensional network of fibrous spectrin molecules which represents a polymerized membrane (on sufficiently short timescales) with a mesh size of $\sim 0.1\text{--}0.2\text{ }\mu\text{m}$. This network has a small but finite shear modulus, $\mu \approx 5 \times 10^{-6}\text{ J m}^{-2}$ (refs 71, 72).

The flickering of red blood cells has been studied experimentally for a long time^{41,73}. From the theoretical point of view, these fluctuations should exhibit a characteristic crossover from fluid-like behaviour with $L_{\perp} \sim L$ on small scales to solid-like behaviour with $L_{\perp} \sim L^{1/2}$ on large scales⁶³. This crossover should

occur on a scale that is comparable to the mesh size of the spectrin network.

Adhesion and renormalized interactions

Adhesion of membranes plays an essential part in many biological and biophysical phenomena⁵². The formation of tissue, for example, is based on the mutual adhesion of cell membranes or on the adhesion of these membranes to a network of macromolecules. On a somewhat smaller scale, many transport processes involve the binding and unbinding of vesicles to and from the membrane surfaces of cells and organelles. This latter process can be used for the delivery of drugs to specific cell types. The construction of biosensors is often based on the binding of membranes to solid surfaces.

The shape of large adhering vesicles can be observed through a light microscope (Figs 2 and 3). Within the contact region between the vesicle and the substrate, the two surfaces are, on average, parallel and separated by a small gap containing water. They then experience a variety of direct interactions arising from the intermolecular forces.

Direct interaction of membranes. Consider two lipid bilayers in water that carry no electric charge, and that have no macromolecules attached to them. Their direct interaction consists of two parts: (1) a strong short-ranged repulsion usually called the hydration interaction⁷⁴—the molecular mechanism underlying this interaction is still controversial⁷⁵ but its repulsive and short-ranged character is well established; and (2) a longer-ranged van der Waals attraction resulting from the polarizabilities of the water and lipid molecules⁷⁶.

The hydration and van der Waals interactions are ‘non-specific’—they are always present for amphiphilic membranes in aqueous solution. In general, the direct interaction includes additional non-specific interactions arising, for example, from electric charges, and ‘specific’ interactions mediated by biologically relevant macromolecules.

Experiments on membrane interactions. The direct interaction between two membranes can be determined experimentally when these membranes are immobilized on molecularly smooth mica surfaces⁷⁷. The force between two such surfaces can be measured accurately as a function of the surface separation.

The interaction between membranes can also be studied in swelling or dilution experiments of lamellar phases consisting of a stack of membranes. For phospholipid bilayers, the intermembrane spacing has been measured as a function of the external pressure, which can be varied over several orders of magnitude⁷⁸. Typical experimental data resemble the results of Monte Carlo simulations, which are shown in Fig. 6. Swelling experiments have also been performed for stacks of surfactant bilayers^{46,47}. The interaction measured in these swelling experiments, however, represents a renormalized interaction which includes the effect of thermally excited shape fluctuations.

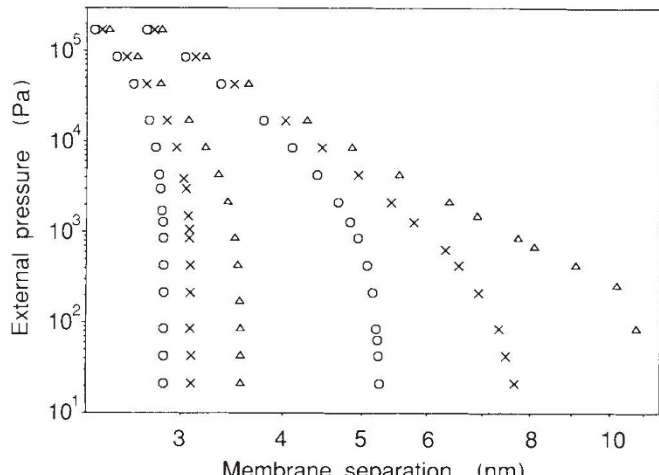


FIG. 6 Monte Carlo simulations of the separation of two interacting fluid membranes as a function of external pressure. The three curves on the right (Hamaker constants $W = 5, 15$ and $25 \times 10^{-21}\text{ J}$) are for room temperature; the three curves on the left represent the behaviour in the absence of shape fluctuations. The difference between these two sets of curves shows the strong renormalization of the direct interaction by shape fluctuations. \triangle , $W = 5 \times 10^{-21}\text{ J}$; \times , $W = 15 \times 10^{-21}\text{ J}$; \circ , $W = 25 \times 10^{-21}\text{ J}$.

Unbinding and adhesion transitions. Thermal shape fluctuations renormalize the direct interaction, increasing its repulsive part^{79,80,37} (see Box B). The renormalized interaction may be attractive or repulsive at large membrane separation, corresponding to a bound or an unbound state of the membranes. These two different states are separated by a phase boundary at which the membranes undergo an unbinding or adhesion transition⁸⁰.

Unbinding transitions were first found theoretically by functional renormalization-group (RG) methods. The RG results imply that two lipid bilayers interacting with realistic intermembrane forces undergo such a transition at a critical unbinding temperature T_u (ref. 80). In addition, the RG calculation predicts that these unbinding transitions are continuous and characterized by universal critical exponents^{60,80-83}. For example, the mean separation, $\langle l \rangle$, of the membrane from the other surface grows continuously as $\langle l \rangle \sim 1/(T_u - T)^\psi$ as the unbinding temperature is approached from below. The critical exponent ψ is universal in the sense that it is independent of the parameters of the direct interaction, and has the exact value $\psi = 1$ for fluid membranes, and the value $\psi \approx 2/3 (< 1)$ for polymerized membranes⁶⁰. Similar transitions also occur when a crumpled membrane is adsorbed onto another surface⁸⁴.

Consider two (or several) membranes that are subject to an external pressure and thus have a finite separation $\langle l \rangle$. The presence of an unbinding transition can then be deduced from the behaviour of $\langle l \rangle$ in the limit of vanishing pressure^{80,85}: for $T < T_u$ and $T > T_u$, the membranes attain a finite and an infinite separation, respectively, as the pressure is decreased to zero. This unbinding transition is in many ways analogous to the wetting transition studied extensively in gas-liquid-surface equilibria³⁷.

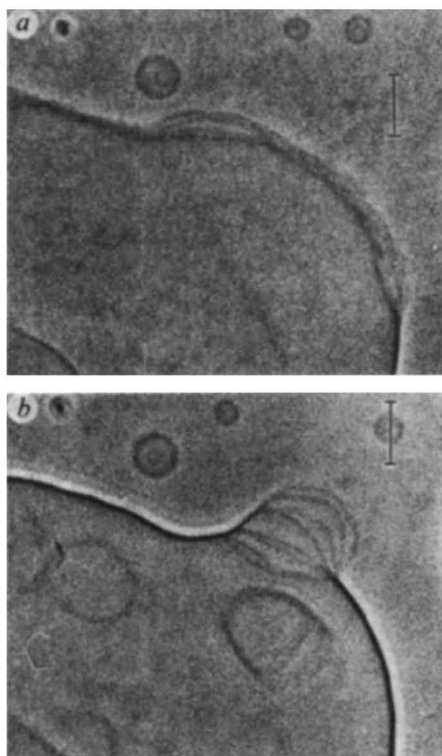


FIG. 7 Unbinding or adhesion transition as observed experimentally for a bunch of lipid bilayers in aqueous solution. *a*, For $T \approx 22.4$ °C, the membranes undulate very strongly, appearing as thick fuzzy lines. *b*, For $T \approx 22.1$ °C, the membranes form a bound state, corresponding to the sharp dark line. The water between the membranes has been squeezed into the large water pocket. The bars represent 10 μm . (Courtesy of W. Helfrich.)

For fluid membranes, the existence of unbinding transitions has been confirmed by recent Monte Carlo simulations^{17,86}. The results shown in Fig. 6 were obtained for two membranes with bending rigidities $\kappa_1 = \kappa_2 = 0.2 \times 10^{-19}$ J that experience realistic hydration and van der Waals interactions and are subject to an external pressure. The different values of the Hamaker constant W in Fig. 6 determine the strength of the van der Waals interaction. Extrapolation of the room-temperature data gives the critical value $W_u \approx 3 \times 10^{-21}$ J: for $W < W_u$, the shape fluctuations overcome the van der Waals attraction and the membranes unbind in the limit of zero pressure. Similar results have been obtained for the unbinding transition of solid-like elastic sheets⁶³ and tethered networks (F. F. Abraham and M. Kardar, preprint, MIT).

Unbinding and adhesion transitions of fluid membranes have also been found in recent experiments with sugar-lipid mem-

Box B. FLUCTUATION INDUCED REPULSION AND RENORMALIZED INTERACTIONS

Consider a fluctuating membrane that adheres to another surface. The entropy of such a bound membrane is reduced by the presence of the second surface. All shape fluctuations of the free membrane that exceed a certain wavelength L_{\max} are inaccessible to the bound membrane. The difference, $\Delta S = S_b - S_f$, between the entropies of the bound and the free state can be estimated by the difference in the number of accessible modes⁹⁰. For a two-dimensional object, the latter difference scales as $-(R/L_{\max})^2$ for large size, R , of the membrane. The excess free energy per unit area arising from the confinement of the shape fluctuations is then given by

$$V_f = -kT\Delta S / R^2 \sim kT / L_{\max}^2 \quad (\text{B.1})$$

which represents a fluctuation-induced repulsion acting between the surfaces.

For a rough membrane, the scale invariance of the shape fluctuations is characterized by $L_\perp \sim \mathcal{A}L^\zeta$ with roughness exponent ζ . \mathcal{A} depends on temperature and on the elastic moduli. If the membrane is bound to another surface at separation l , this scale invariance holds only up to $L_\perp \sim l$ and $L = L_{\max} \sim (l/\mathcal{A})^\tau$ with $\tau = 2/\zeta$. It then follows from (B.1) that the fluctuation-induced repulsion is given by³⁷ $V_f \sim kT\mathcal{A}^\tau/l^2$. For fluid membranes with $\tau = 2$ and $\mathcal{A} = (kT/\kappa)^{1/2}$, such a repulsive interaction was first predicted by Helfrich⁷⁹.

Some information about the renormalization of the direct interaction $V(l)$ can be obtained from a simple superposition of $V(l)$ and $V_f(l)$. To study the properties of unbinding or adhesion transitions, however, one has to use a more systematic theoretical approach which is provided by renormalization-group (RG) methods.

Roughly speaking, the direct interaction $V(l)$ represents the interaction between two surface segments of linear size a , the smallest wavelength available to the shape fluctuations. Within the RG approach, one then calculates the effective interaction, $V(|t|)$, between two segments of linear size $a_t = a \exp(t)$ with $t > 0$. This interaction contains all fluctuations of wavelength L with $a < L < a_t$. As t is increased, one successively includes more shape fluctuations and thus obtains the effective interaction on increasingly larger scales.

The first RG method to be used to calculate the renormalized interaction⁸⁰ was an extension of Wilson's approximate recursion relation⁹¹ and was applied previously to wetting phenomena^{37,92}. This RG scheme leads to the differential flow equation

$$\partial V / \partial t = 2V + \zeta \partial V / \partial l + \frac{1}{v} \partial V / \partial l^2 \quad (\text{B.2})$$

for the renormalized interaction $V(|t|)$, where the scale factors v and a_t depend on the temperature and on the microscopic scale a . This RG transformation has a line of fixed points, $V^*(l)$, characterized by $\partial V^*/\partial t = 0$ (refs 60, 81-83). The RG flow in the vicinity of these fixed points then determines the critical behaviour at the unbinding transitions—providing, for example, the critical exponent ψ for the mean separation $\langle l \rangle$.

The above theory does not include any hydrodynamical effects. The fluctuating membrane is, however, coupled to overdamped surface waves in the aqueous medium^{41,93,94}. The amplitude of these waves decays as $\exp(-qz)$ with distance z from the membrane. This is a long-ranged effect which should lead to $L_{\max} \sim l$ and thus, according to (B.1), to an effective repulsion $V_f \sim T/l^2$ between the surfaces.

branes⁸⁷, in which bunches of membranes were observed by light microscopy (Fig. 7). Above a characteristic unbinding temperature, T_u , these membranes are unbound and exhibit strong undulations, appearing as thick fuzzy lines in Fig. 7a. As the sample is cooled below T_u , the membranes suddenly form a bound state, visible in Fig. 7b as the sharp dark line. Adhesion of the membranes drives the water between them into compact pockets. A similar transition may have been observed in experiments on phospholipid bilayers, in which the swelling behaviour was studied for different levels of salinity⁸⁸.

For $T > T_u$, adhesion of membranes can be induced by a lateral tension, Σ , which acts to suppress the shape fluctuations. Such a tension-induced adhesion has been observed for fluid lecithin membranes⁸⁹. In the limit of small Σ , the membrane separation grows as $\langle l \rangle \sim 1/\Sigma^{1/2}$ which represents a superuniversal scaling law, as it holds for fluid, polymerized and hexatic membranes¹⁷.

Summary and outlook

The conformational behaviour of membranes continues to provide many challenging problems for future research. In the context of vesicle shapes, one poorly understood phenomenon is 'blebbing'—the formation of a long necklace of small vesicles which is expelled from a larger one (refs 4, 95; L. Miao *et al.*, preprint, Simon Fraser Univ.). As far as shape fluctuations are concerned, there is still no clear understanding of the large-scale behaviour of fluid membranes, which may remain uncrumpled as a result of self-avoidance. Likewise, it remains to be seen

whether a realistic model membrane can be found that undergoes a crumpling transition. Experimentally, it is important to probe the whole range of length scales involved in these fluctuations. Some very promising tools are X-ray and neutron scattering. These methods should also be useful for systematic studies of unbinding and adhesion transitions.

In a more general context, another set of puzzles is provided by the very dynamic features of the membrane surfaces of biological cells and organelles. These membranes continuously form and expel small vesicles towards the exterior and the interior of the various compartments⁵². These processes, called respectively budding and endocytosis, look rather similar to the shape transformations of lipid vesicles shown in Fig. 1. Even though budding and endocytosis of biomembranes are typically induced by local changes in the membrane structure, these processes will still fit into the conceptual framework described here if they do not depend crucially on the release of metabolic energy. On the other hand, some form of metabolic energy is certainly involved in the heavy traffic of vesicles which shuttle between different compartments of the cell.

Finally, membranes must have played a crucial role in the origin of life. One may postulate that cellular life began with a vesicle containing just the right mixture of polymers. But where did the amphiphilic molecules that formed the first vesicle come from? □

Reinhard Lipowsky is at the Institut für Festkörperforschung, Forschungszentrum Jülich, 5170 Jülich, Germany.

1. Bangham, A. D. & Horne, R. W. *J. molec. Biol.* **8**, 660–668 (1964).
2. Lasic, D. D. *Biochem. J.* **256**, 1–11 (1988).
3. Sackmann, E., Duwe, H. P. & Engelhardt, H. *Faraday Discuss. Chem. Soc.* **81**, 281–290 (1986).
4. Berndl, K., Kaes, J., Lipowsky, R., Sackmann, E. & Seifert, U. *Europhys. Lett.* **13**, 659–664 (1990).
5. Canham, P. B. *J. theor. Biol.* **26**, 61–81 (1970).
6. Helfrich, W. Z. *Naturforsch.* **28c**, 693–703 (1973).
7. Evans, E. *Biophys. J.* **14**, 923–931 (1974).
8. Duwe, H. P., Kaes, J. & Sackmann, E. *J. Phys. Fr.* **51**, 945–962 (1990).
9. Mutz, M. & Helfrich, W. *J. Phys. Fr.* **51**, 991–1002 (1990).
10. Harbich, W. & Helfrich, W. Z. *Naturforsch.* **34a**, 1063–1065 (1979).
11. Fromherz, P., Röcker, C. & Rüppel, D. *Faraday Discuss. Chem. Soc.* **81**, 39–48 (1986).
12. Deuling, H. J. & Helfrich, W. *J. Physique* **37**, 1335–1345 (1976).
13. Svetina, S. & Žeks, B. *Eur. Biophys. J.* **17**, 101–111 (1989).
14. Seifert, U., Berndl, K. & Lipowsky, R. *Phys. Rev. A* (submitted).
15. Evans, E. & Needham, D. *J. phys. Chem.* **91**, 4219–4228 (1987).
16. Seifert, U. & Lipowsky, R. *Phys. Rev. A* **42**, 4768–4771 (1990).
17. Lipowsky, R. & Seifert, U. in *Proc. 13th Int. Liquid Crystal Conf.* (Vancouver, 1990).
18. Zimmerberg, J. *Biosci. Rep.* **7**, 251–268 (1987).
19. Helfrich, W. & Harbich, W. in *Physics of Amphiphilic Layers* (eds Meunier, J., Langevin, D. & Boccardo, N.) 58–63 (Springer, Berlin, 1987).
20. Czaja, C., Jekutin, G., Rothenhäusler, B. & Gaub, H. E. in *Biosensors Int. Workshop* 1987 (ed. Schmid, R. D.) 339–340 (VCH Verlag, Weinheim, 1988).
21. Cevc, G., Fenzi, W. & Sigi, L. *Science* **249**, 1161–1163 (1990).
22. Hauser, H., Gains, N. & Müller, M. *Biochemistry* **22**, 4775–4781 (1983).
23. Talmon, Y., Evans, D. F. & Ninham, B. W. *Science* **221**, 1047–1048 (1983).
24. Gabriel, N. E. & Roberts, M. F. *Biochemistry* **23**, 4011–4015 (1984).
25. Kaler, E. W., Murthy, A. K., Rodriguez, B. E. & Zasadzinski, J. A. N. *Science* **245**, 1371–1374 (1989).
26. Gunning, B. E. S. *Protoplasma* **60**, 111–130 (1965).
27. Luzzati, V., Tardieu, A., Gulik-Krzywicki, T., Rivas, E. & Reiss-Husson, F. *Nature* **220**, 485–488 (1968).
28. Scriven, L. E. *Nature* **263**, 123–125 (1976).
29. Harbich, W., Servuss, R. M. & Helfrich, W. Z. *Naturforsch.* **33a**, 1013–1017 (1978).
30. Longley, W. & McIntosh, J. *Nature* **303**, 612–614 (1983).
31. Dubois-Violette, E. & Pansu, B. (eds) *Geometry and Interfaces Proc. Aussois 1990*, *J. Phys. Colloq. France* **7** (1990).
32. Anderson, D. M., Davis, H. T., Nitsche, J. C. C. & Scriven, L. E. in *Physics of Amphiphilic Layers* (eds Meunier, J., Langevin, D. & Boccardo, N.) 130 (Springer, Berlin 1987).
33. Karcher, H. *Manusc. math.* **64**, 291–357 (1989).
34. Cates, M. E., Roux, D., Andelman, D., Milner, S. & Safran, S. *Europhys. Lett.* **5**, 733–739 (1988); *erratum*, **7**, 94 (1988).
35. Huse, D. & Leibler, S. *J. Phys. Fr.* **49**, 605–621 (1988).
36. Porte, G., Appell, J., Bassereau, P. & Marignan, J. *J. Phys. Fr.* **50**, 1335–1347 (1989).
37. Lipowsky, R. *Physica Scripta* **T29**, 259–264 (1989); and in *Fundamental Problems in Statistical Mechanics* VII (ed. van Beijeren, H.) 139–170 (North-Holland, Amsterdam, 1990).
38. Singer, S. J. & Nicolson, G. L. *Science* **175**, 720–731 (1972).
39. Kornberg, R. D. & McConnell, H. M. *Proc. natn. Acad. Sci. U.S.A.* **68**, 2564–2568 (1971).
40. Clegg, R. M. & Vaz, W. L. C. in *Progress in Protein-Lipid Interactions* (eds by Watts, A. & De Pont, J. J. H. M.) 173–229 (Elsevier, Amsterdam, 1985).
41. Brochard, F. & Lennon, J. F. *J. Phys. (Paris)* **36**, 1035–1047 (1975).
42. de Gennes, P.-G. & Taupin, C. *J. phys. Chem.* **88**, 2294–2304 (1982).
43. Helfrich, W. *J. Physique (Paris)* **46**, 1263–1268 (1985).
44. Peliti, L. & Leibler, S. *Phys. Rev. Lett.* **54**, 1690–1693 (1985).
45. Di Miglio, J. M., Dvolaitzky, M., Leger, L. & Taupin, C. *Phys. Rev. Lett.* **54**, 1686–1689 (1985).
46. Larche, F., Appell, J., Porte, G., Bassereau, P. & Marignan, J. *Phys. Rev. Lett.* **56**, 1700–1703 (1986).
47. Safinya, C. R. *et al.* *Phys. Rev. Lett.* **57**, 2718–2721 (1986).
48. Baumgärtner, A. & Ho, J.-S. *Phys. Rev. A* **41**, 5747–5750 (1990).
49. de Gennes, P. G. *Scaling Concepts in Polymer Physics* (Cornell University Press, New York, 1979).
50. Kantor, Y., Kardar, M. & Nelson, D. R. *Phys. Rev. A* **35**, 3056–3071 (1987).
51. Leibler, S., Singh, R. R. P. & Fisher, M. E. *Phys. Rev. Lett.* **59**, 1989–1992 (1987).
52. Alberts, B. *et al.* *Molecular Biology of the Cell* (Garland, New York, 1983).
53. Bader, H., Dorn, K., Hupfer, B. & Ringsdorf, H. *Adv. Polymer Sci.* **64**, 1–62 (1985).
54. Sackmann, E. *et al.* *Bunsenges. Phys. Chem.* **89**, 1198–1208 (1985).
55. Landau, L. D. & Lifschitz, E. M. *Theory of Elasticity* (Pergamon, New York, 1970).
56. Nelson, D. R. & Peliti, L. *J. Physique* **48**, 1085–1092 (1987).
57. Kantor, Y. & Nelson, D. *Phys. Rev. Lett.* **58**, 2774–2777 (1987).
58. David, F. & Guitter, E. *Europhys. Lett.* **5**, 709–713 (1988).
59. Nelson, D. R., Piran, T. & Weinberg, S. (eds) *Statistical Mechanics of Membranes and Surfaces* (World Scientific, Singapore, 1988).
60. Lipowsky, R. *Europhys. Lett.* **7**, 255–261 (1988).
61. Leibler, S. & Maggs, A. *Phys. Rev. Lett.* **63**, 406–409 (1989).
62. Abraham, F. F. & Nelson, D. R. *Science* **249**, 393–397 (1990).
63. Lipowsky, R. & Girardet, M. *Phys. Rev. Lett.* **65**, 2893–2896 (1990).
64. Plischke, M. & Boal, D. *Phys. Rev. A* **38**, 4943–4945 (1988).
65. Abraham, F. F., Rudge, W. E. & Plischke, M. *Phys. Rev. Lett.* **62**, 1757–1759 (1989).
66. Ho, J.-S. & Baumgärtner, A. *Phys. Rev. Lett.* **63**, 1324 (1989).
67. Sackmann, E., Fischer, A. & Frey, W. in *Physics of Amphiphilic Layers* (eds Meunier, J., Langevin, D. & Boccardo, N.) 25–37 (Springer, Berlin, 1987).
68. Seung, H. S. & Nelson, D. R. *Phys. Rev. A* **38**, 1005–1018 (1988).
69. David, F., Guitter, E. & Peliti, L. *J. Physique* **48**, 2059–2066 (1987).
70. Elgsaeter, A., Stokke, B. T., Mikkelsen, A. & Branton, D. *Science* **234**, 1217–1223 (1986).
71. Waugh, R. & Evans, E. *Biophys. J.* **26**, 115–131 (1979).
72. Engelhardt, H. & Sackmann, E. *Biophys. J.* **54**, 495–508 (1988).
73. Zilker, A., Engelhardt, H. & Sackmann, E. *J. Phys. (Paris)* **48**, 2139–2151 (1987).
74. Rand, R. P. & Parsegian, V. A. *Biochim. biophys. Acta* **988**, 351–376 (1989).
75. Israelachvili, J. N. & Wernersson, H. *Langmuir* **6**, 873–876 (1990).
76. Israelachvili, J. N. *Intermolecular and Surface Forces* (Academic, London, 1985).
77. Marra, J. & Israelachvili, J. N. *Biochemistry* **24**, 4608–4618 (1985).
78. Parsegian, V. A., Fuller, N. & Rand, R. P. *Proc. natn. Acad. Sci. U.S.A.* **76**, 2750–2754 (1979).
79. Helfrich, W. Z. *Naturforsch.* **33a**, 305–315 (1978).
80. Lipowsky, R. & Leibler, S. *Phys. Rev. Lett.* **56**, 2541–2544 (1986); *Erratum* **59**, 1983 (1987).
81. Lipowsky, R. *Phys. Rev. Lett.* **62**, 704–707 (1989).
82. Grotenhuis, S. & Lipowsky, R. *Phys. Rev. A* **41**, 4574–4577 (1990).
83. David, F. & Leibler, S. *Phys. Rev. B* **41**, 12926–12929 (1990).
84. Lipowsky, R. & Baumgärtner, A. *Phys. Rev. A* **40**, 2078–2081 (1989).
85. Leibler, S. & Lipowsky, R. *Phys. Rev. B* **35**, 7004–7009 (1987).
86. Lipowsky, R. & Zielska, B. *Phys. Rev. Lett.* **62**, 1572–1575 (1989).
87. Mutz, M. & Helfrich, W. *Phys. Rev. Lett.* **62**, 2881–2884 (1989).
88. Lis, L. J., Lis, W. T., Parsegian, V. A. & Rand, R. P. *Biochemistry* **20**, 1771–1777 (1981).
89. Servuss, R. M. & Helfrich, W. *J. Phys. France* **50**, 809–827 (1989).
90. Frenkel, J. *Kinetic Theory of Liquids* (Clarendon, Oxford, 1946).
91. Wilson, K. G. *Phys. Rev. B* **4**, 3184–3205 (1971).
92. Lipowsky, R. & Fisher, M. E. *Phys. Rev. B* **36**, 2126–2141 (1987).
93. Schneider, M. B., Jenkins, J. T. & Webb, W. W. *J. Phys. (Paris)* **45**, 1457–1472 (1984).
94. Milner, S. T. & Safran, S. A. *Phys. Rev. A* **36**, 4371–4379 (1987).
95. Evans, E. & Rawicz, W. *Phys. Rev. Lett.* **64**, 2094–2097 (1990).
96. do Carmo, M. *Differential Geometry of Curves and Surfaces* (Prentice-Hall, Englewood Cliffs, 1976).

ACKNOWLEDGEMENTS. I thank all my collaborators for enjoyable and fruitful interactions. This work has been partially supported by the Sonderforschungsbereich 266 der Deutschen Forschungsgemeinschaft.